Supplementary Table. *Paramecium* specific primers used in this study

Oligo Name	IES	Gene	sequence (5'-3')	GenBank coordinates	orientation
G10	51G4404	*G*[51]	AAAGGCTAATTTGGATGAATGAGCATTAAATC	7459-7428 (AJ010441)	-
G11			GGACTACTTTTGAAATTGAATTATAACAAAGGC	7486-7454	-
G13			TGCATATGTTACTGGAACTGGATTGGTAGC	7293-7322	+
G18			ACTGTTGCTACACATTGTGCATATGTTACT	7276-7305	+
51A1416-5'	51A1416	*A*[51]	TGCTTCTGGGATTCTGCTAGTTCAAGTTGC	2460-2489 (L26124)	+
51A1835-5'(3)	51A1835	*A*[51]	GGTTGCGTAACACTTCCTCTTAAATGTGAG	2849-2878	+
51A1835-5'(4)			GAAGTCTAATGGATAACCTTGTGGATGGAC	2908-2937	+
51A1835-3'(4)			AGACAAGTAGGGAATCCACTTCTAGTAATC	3184-3155	-
51A1835-3'(3)			GTAGTACAAGATTTTTCGACACAAGTTGAG	3229-3200	-
51A2591-5'	51A2591	*A*[51]	ACACCAAGCGAAACATGCACAGTCG	3747-3771	+
51A2591-3'			TTTTATGGCATTAAGCTTGTGTCAT	4222-4198	-
51A2591-16			AATTGTAAATTGACTTCAGCAAATAAAAAA	3621-3650	+
51A2591-17			ATGTGTTTGGACTGGATTGGCATGTAGAAG	3650-3679	+
51A6649-11(2)	51A6649	*A*[51]	GGATGCGTTACTAAATCCTCATGCTCAGCT	9094-9123	+
51A6649-12(2)			ACTGCACCTCTAACTTTAACAAGCGAAGCA	9019-9048	+
51A6649-17(2)			TGATCCTTCTATGCAAGCTGCTCTTACGGT	9718-9689	-
51A6649-18(2)			ATCCATAAGCATGGTCCGTTTGATCCTTCT	9738-9709	-
sm19-2	sm19-576	*sm19*	AATTAAGCAAGAAAAGAAATAGAAAAAACC	677-706 (AJ272425)	+
sm19-3			CTACAATAATGAGTCTAGCTGGTGGCACTG	726-755	+
sm19-4			GACAAGATCCTATATATTCATTTACATTTG	1028-999	-
sm19-6			ACTTAACATTTAATATATCCTGTCATTCTC	958-929	-

+ or - : Oligonucleotides are oriented relatively to the transcriptional direction of the genes.

Gratias et al. Figure S1

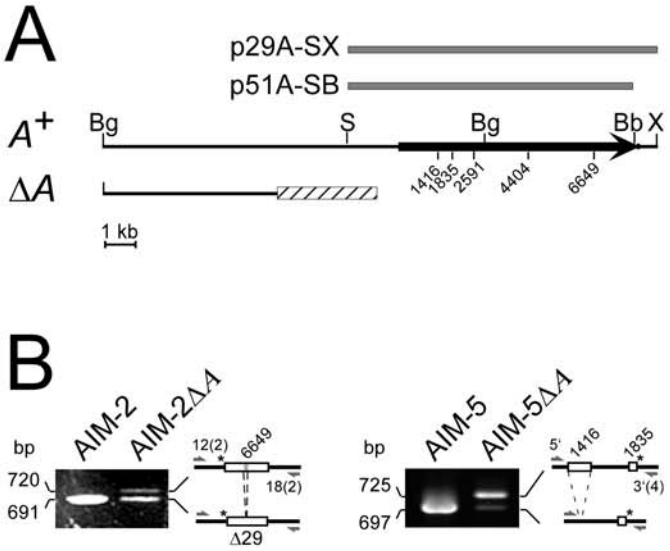

Gratias et al. Figure S2

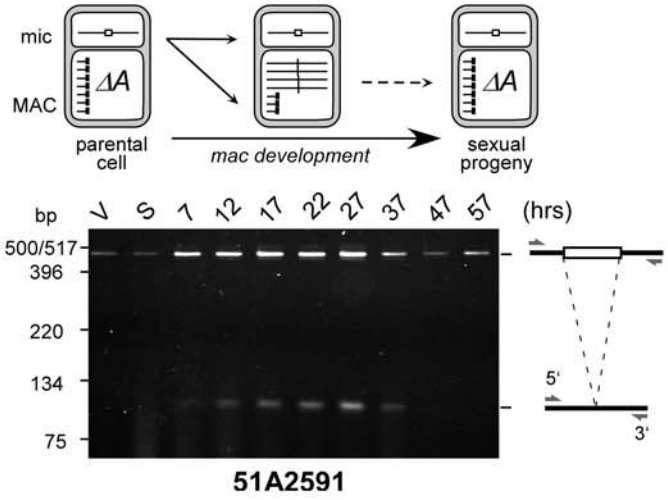

Gratias et al. Figure S3

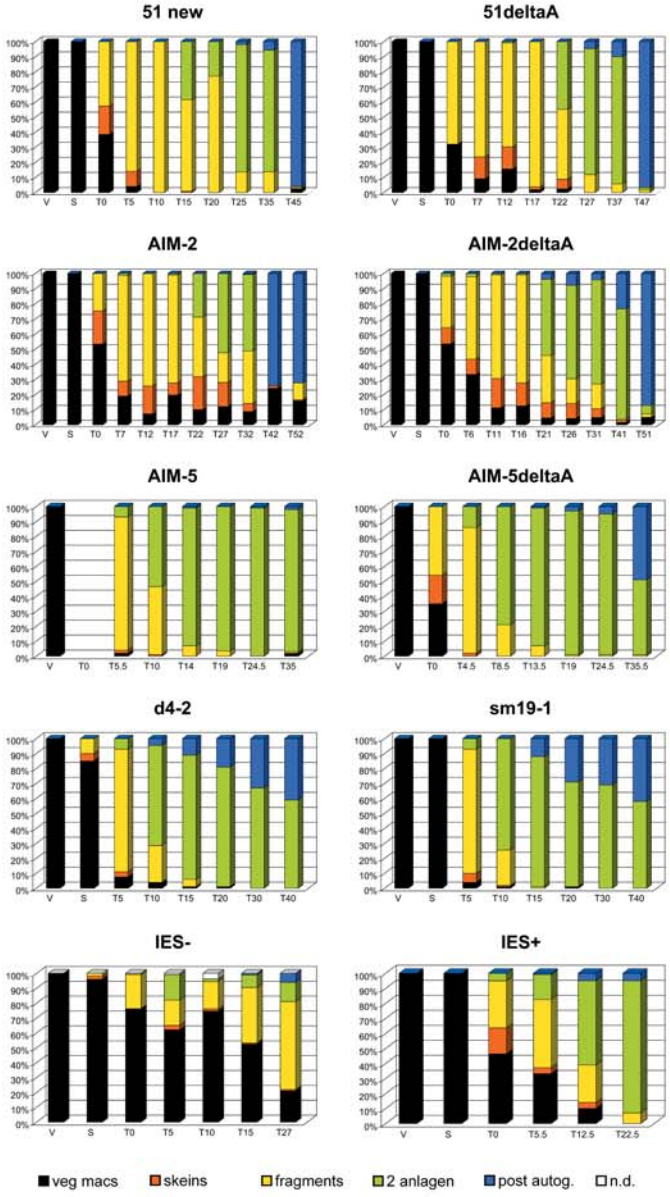

Gratias et al. Figure S4

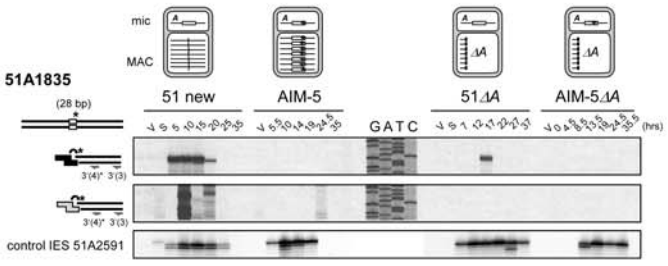

Gratias et al. Figure S5

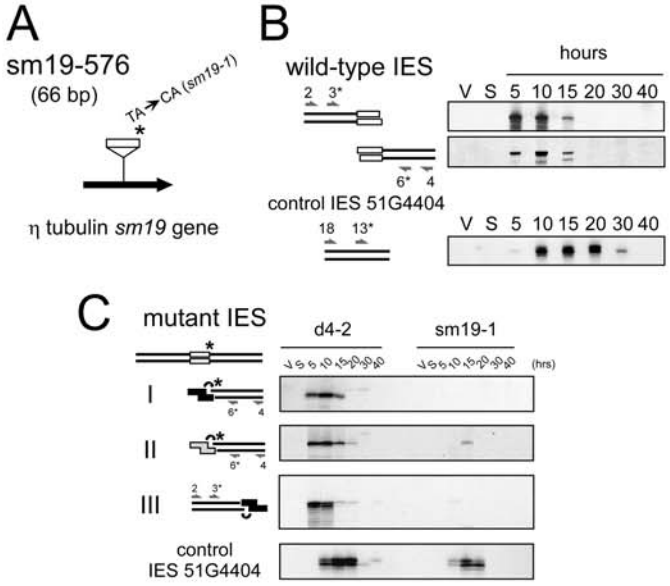

Gratias et al. Figure S6

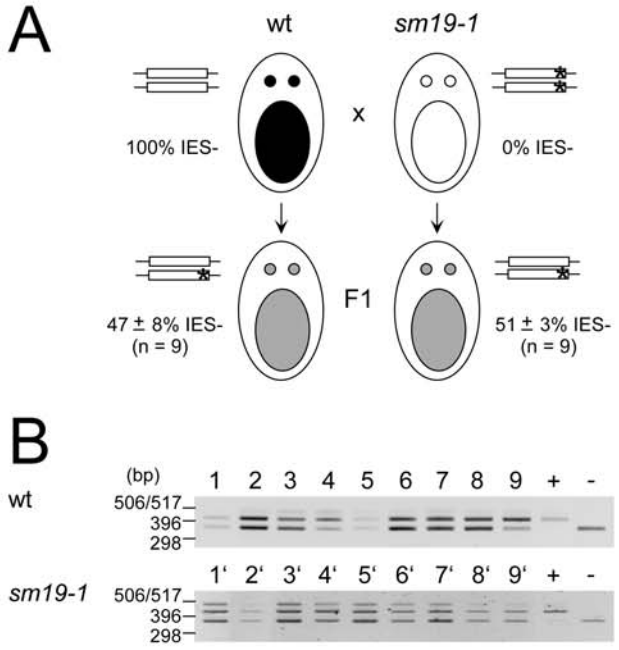

Legends to Supplementary Figures

Figure S1 Construction of the 51Δ*A*, AIM-2Δ*A* and AIM-5Δ*A* macronuclear variants. **(A)** Schematic map of the macronuclear locus carrying the *A* gene (black arrow). Relevant restriction sites are indicated (Bb : *Bbs*I ; Bg: *Bgl*II; S: *Sal*I; X: *Xho*I). The structure of Δ*A* macronuclear deletions is shown, with the variable telomere addition region represented by a hatched box. Cloned fragments injected for the induction of Δ*A* macronuclear deletions are shown as gray lines. The position of the IESs analyzed in this study is shown on the map. **(B)** Estimation of the copy number of mutant IESs 51A6649 (left panel) and 51A1835 (right panel) in the vegetative macronucleus of variant strains AIM-2Δ*A* and AIM-5Δ*A*, respectively. PCR primers are indicated on each diagram. Electrophoresis was performed on 3% NuSieve agarose gels run in 1X TBE buffer. Left panel: the macronuclear form of mutant IES 51A6649 (bottom) differs from its micronuclear form (top) by the absence of an internal 29-bp IES. The AIM-2Δ*A* variant exhibits a 1.3 ratio in its relative macro- to micronuclear copy numbers of IES 51A6649. Given that *P. tetraurelia* harbors two diploid micronuclei (i.e. 4 micronuclear copies of the IES per cell), this leads to 5.2 copies of IES 51A6649 in the macronucleus of the vegetative parental strain. Taking into account the ~800n ploidy of the macronucleus, this corresponds to ~6.5 x 10^{-3} IES copies per haploid genome (cphg), which is well below the threshold (0.1 cphg) above which maternal inhibition of excision is observed for this IES (Duharcourt *et al.* (1998) Mol. Cell. Biol. 18: 7075-7085). Right panel: the micronuclear fragment (top) includes mutant IES 51A1835 and neighboring IES 51A1416, which is excised from the macronuclear fragment (bottom). Based on the same calculations as for AIM-2Δ*A*, an even lower 0.24 macro- to micronuclear ratio (i.e. 1.2 x 10^{-3} cphg) was estimated for IES 51A1835 in the AIM-5Δ*A* variant.

Figure S2 Excision of IESs 51A2591 during autogamy of a 51Δ*A* macronuclear variant. Primers used for amplification of the excised (bottom band) and non-excised (top band) forms are indicated. PCR products amplified with the Expand Long Template PCR System were separated in a 3% NuSieve GTG agarose gel run in 0.5X TBE buffer. IES excision can be visualized directly, as demonstrated by the appearance of a 106-bp band in the T7-T37 samples. DNA sequencing confirmed that the corresponding excision junctions are precise (not shown). These disappear at the latest time-points (T47-T57), as a result of maternally controlled macronuclear deletion of the *A* gene.

Figure S3 Progression of autogamy in starved cultures of strains 51 new, 51Δ*A*, AIM-2, AIM-2Δ*A*, AIM-5, AIM-5Δ*A*, d4-2, d4-2 *sm19-1*, a wt cell line from stock 51 new (IES^-) and its IES^+ macronuclear variant. At each time-point, at least 100 cells were stained with DAPI. V : vegetative cells ; S : starved cells with intact macronuclei. Time-points (in hours) are indicated below the x-axis of each graph. Cells with a single new macronucleus and variable numbers (~ 2 to 15) of fragments were considered as post-autogamous. In the experiment with the IES^- cell line, « n.d. » refers to cells exhibiting unusual patterns.

Figure S4 Effect of a germline TA to TG mutation at the right end of IES 51A1835 on the cleavage of the mutant end. Top : schematic representation of the *A* locus in the maternal macronucleus of each strain, with IES 51A1835 drawn as a white box and its mutant end marked with an asterisk. Bottom panels : LMPCR detection of broken chromosome ends in strains 51 new, AIM-5, 51ΔA and AIM-5ΔA, using linkers I'/(ATAT)J' (wt: shown in black for top panel) or I'/(ACAT)J' (mutant: shown in grey for middle panel). LMPCR primers are represented by arrows. As a size marker for both panels, we ran a DNA sequencing ladder of the cloned micronuclear locus. The same oligonucleotide was used for primer extension and

sequencing. Bottom panel: double strand breaks at the left end of control IES 51A2591 analyzed with linker I'/(GTAT)J' and oligonucleotides 51A2591-16 and 51A2591-17 for PCR and primer extension, respectively. Autogamy time-points are indicated. Note that the mutant linker is not able to ligate to the wild-type broken end : only non-specific LMPCR products are revealed in 51 new, while no band is detected in 51Δ*A*.

Figure S5 Analysis of double strand cleavages at the ends of 66-bp IES sm19-576. **(A)** Map of mutant IES in stock d4-2 *sm19-1*, with a TA to CA mutation at its right end (*). **(B)** Control experiment showing the detection of single-end cleaved IES sm19-576 during autogamy of wild-type strain d4-2. Linkers I'/(GTAG)J' and I'/(GTAT)J' were used for LMPCR analysis of the right (top panel) and left (middle panel) ends, respectively. **(C)** LMPCR detection of broken chromosome ends at the mutant and wild-type ends of IES sm19-576 during autogamy of strain d4-2 *sm19-1*. Analysis of the mutant right end was carried out with linkers I'/(CTAC)J' (panel I) or I'/(CTGC)J' (panel II). LMPCR linker I'/(ATAC)J' was used for the analysis of IES sm19-576 wild-type left end (panel III). In (B) and (C), bottom panels show the detection of double strand breaks at the left end of control IES 51G4404 analyzed with linker I'/(GTAT)J' and oligonucleotides 51G18 and 51G13 for PCR and primer extension, respectively. LMPCR primers are indicated by arrows and linkers by z-shaped boxes.

Figure S6 Excision of wild-type IES sm19-576 in F1 heterozygotes from a d4-2 x d4-2 *sm19-1* cross. (A) Schematic diagram of the cross. The two copies of IES sm19-576 in each diploid micronucleus are displayed as white boxes next to each cell, with the mutant end marked with an asterisk. The overall % of IES sm19-576 excision in each macronucleus is indicated for each homozygous parent (top: d4-2 (wt) and d4-2 *sm19-1*) and its respective F1 progeny (bottom: average values calculated on each side of the cross for F1 heterozygotes issued from 9 independent conjugating pairs). (B) PCR analysis of IES sm19-576 excision in F1 progeny from 9 independent conjugating pairs. Primers sm19-2 and sm19-4 were used to amplify excised and non excised IES forms from total genomic DNA of vegetative cells and PCR products were resolved in 3% NuSieve agarose electrophoresis gels (+: mutant d4-2 *sm19-1* parent; -: wild-type d4-2 parent). Quantification of the IES- (352 bp) and IES+ (418 bp) forms was performed following ethidium bromide staining. In some lanes, a slow migrating species was shown to be an IES+ / IES- heteroduplex formed during the PCR reaction: it was taken into account for the calculation of the % of IES excision in each individual F1 (average value displayed in A).